sciendo

LATVIAN JOURNAL OF PHYSICS
AND TECHNICAL SCIENCES
2024, N 2

DOI: 10.2478/lpts-2024-0009

# TOWARDS SCALABLE SYNTHESIS OF $TiSe_2$ AND $VSe_2$ THIN FILMS

K. Kadiwala*, E. Dipans, L. Dipane, E. Butanovs, B. Polyakov

Institute of Solid State Physics, University of Latvia,
8 Kengaraga Str., Riga LV-1063, LATVIA
*e-mail: kevon.kadiwala@cfi.lu.lv

Transition metal dichalcogenides (TMDs), specifically those involving V and Ti, possess fascinating material properties, making them interesting candidates for scientific studies. The existing growth methods of these materials are typically limited by scalability – either low yield or high cost. Here, we propose an alternative 2-step method valid for scalable production. In the first step, precursor films of Ti / V are deposited using magnetron sputtering, followed by the second step of selenization of these samples using elemental Se in a vacuum-sealed quartz ampoule for conversion to their respective diselenide material. Synthesized films are characterised using scanning electron microscope (SEM), energy dispersive X-ray spectroscopy (EDX), X-ray diffraction (XRD) and X-ray photoelectron (XPS). The method demonstrated here can be used to increase the active surface area of $TiSe_2$ and $VSe_2$ for their potential catalytic and HER applications using nanostructured substrates, while also providing an opportunity for scalable synthesis of films that can be extended to synthesize other TMDs as well.

***Keywords:*** *Magnetron sputtering, thin films, titanium diselenide, transition metal dichalcogenides, vanadium diselenide.*

## 1. INTRODUCTION

Transition metal dichalcogenides (TMDs) exhibit many scientifically and technologically important properties; therefore, since the 20th century they are being studied with a lot more focus and interest [1]–[5]. Their adaptability and unique properties due to their anisotropy and compatibility with emerging technologies have positioned them at the forefront of research and innovation in the fields ranging from electronics and energy to quantum computing and biomedicine [1]–[6]. Among these TMD materials, titanium diselenide ($TiSe_2$) [7], [8] and vanadium diselenide ($VSe_2$) [9], [10] have attracted significant attention. Many recent studies [11], [13]–[19] have

shown that $TiSe_2$ and $VSe_2$ materials have a charge density wave property. They are remarkable materials with a wide range of potential applications in areas such as thermoelectricity, energy storage, and nanoelectronics [4], [20]–[26]. $VSe_2$ and $TiSe_2$ materials are highly promising for catalysts and HER applications, as it has been reported before in multiple studies [27]–[32]. Overall, for these two TMDs, their charge density wave transition, outstanding thermoelectric properties, and catalytic potential make them versatile materials, which hold promises for various cutting-edge technologies [33], [34], [2], [15], [26], [35].

One of the main challenges in terms of application when it comes to TMD materials such as $TiSe_2$ or $VSe_2$ is their production on a larger scale than a few microns in controllable geometry. In general, when studies related to these materials are performed, these materials are obtained using mechanical or chemical exfoliation of bulk crystals [3], [5], [9]. When such an approach is used, it results in small flakes with inconsistent thickness, no repeatability, poor control over size and shape [3], [5], [21]. The other alternative to create large-area films of these materials is through molecular beam epitaxy (MBE) in an ultrahigh vacuum (UHV) environment [12], [18], [23], [36]. Although this method provides the best quality of the material, it is not a feasible approach for any application-oriented growth of these materials because it is an extremely slow and costly technique. It is advantageous to develop a more straightforward method for growth of such materials. In recent years, ambient-pressure chemical vapour deposition (CVD) has been successfully employed to produce thin layers of semiconducting transition metal dichalcogenides (TMDs), like $MoS_2$ and $WSe_2$ [37], [38]. However, the experimental synthesis of $TiSe_2$ through conventional CVD methods has proven to be challenging [17], where for $VSe_2$ the synthesis process has been shown with success in the synthesis of the material but with random growth of a few micron scale crystals with no continuity over a large area [39].

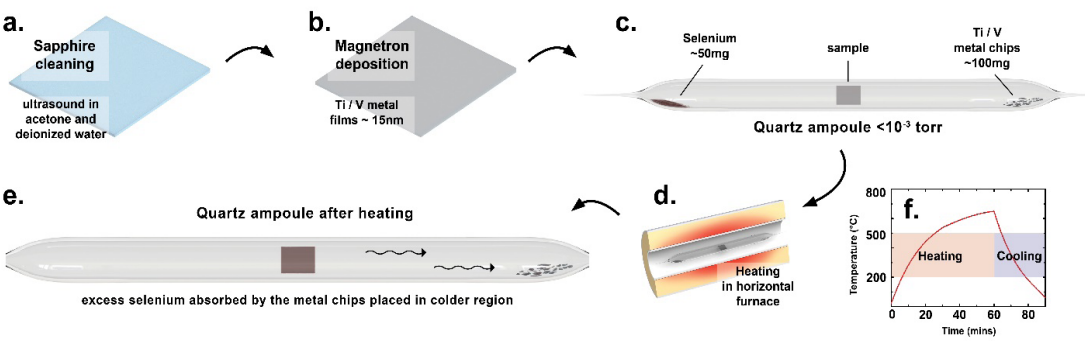


*Fig. 1.* Graphical illustration of the methodology used here to synthesize $TiSe_2$ and $VSe_2$ thin films starting from (a) substrate cleaning in acetone and DIW using ultrasound for 5 min each, followed by (b) deposition of Ti / V metal film using magnetron sputtering; (c) sample was placed in a quartz ampoule with Se powder and respective metal chips in the shown configuration; (d) ampoules were heated up using a horizontal furnace; (e) after heating the ampoule, no excess selenium vapour was found near edges of any ampoules; (f) heating cycle of an ampoule, shown with ramp rate of heating and cooling.

In this study, we present an alternative approach to growth of such materials but on a larger scale that has never been demonstrated before. The present study demonstrates a 2-step process for the synthesis of $TiSe_2$ and $VSe_2$. To start, deposition of metal precursor films is done using magnetron sputtering followed by annealing them in Se vapour atmosphere in a sealed quartz ampoule. Using magnetron sputtering for the deposition of precursor films allows us to deposit them on large surface areas, and we have used it to cover our centimetre scale substrates used here in this study. The same approach could also be used for non-flat surfaces (e.g., nanostructures) to increase their surface area and enhance their properties for their potential applications in catalysis, sensors etc.

## 2. EXPERIMENTAL DETAILS

To synthesize $TiSe_2$ and $VSe_2$ thin films, the methodology used was analogous. We approached the goal of synthesizing these materials in two steps: first, we deposited the precursor metal films using magnetron sputtering and then converted these films to their respective diselenide using sealed quartz ampoules with below atmospheric pressure (Fig. 1). Sacrificial precursor films of ~15nm Ti / V metal were deposited on 10x10 mm cut and cleaned sapphire (r-plane, Biotain Crystal Co.) by DC magnetron sputtering of metallic Ti / V targets in Ar atmosphere ($3 \cdot 10^{-3}$ torr, 30 sccm Ar, at 100 W DC power), which was followed by the process of making ampoules for these samples. For our experiments, the ampules were made from quartz tubes of 13 mm OD with wall thickness of 1 mm and length of $120 \pm 10$ mm, which were loaded with Ti / V metal covered sapphire substrates, Se powder (~50mg) and grinded Ti / V metal chips (~100mg) to absorb any residue of selenium near the edges of an ampoule with inside vacuum pressure being $<10^{-3}$ torr. Using a horizontal open-end tube reactor, these ampoules were heated up to 650 °C, 700 °C and 750 °C in an hour followed by rapid cooling of these ampoules to ambient temperature (Fig. 1f).

The synthesized films were studied using an optical microscope as well as under a scanning electron microscope (SEM-FIB Lyra, Tescan, 12kV) for their surface morphology. Using the same tool, elemental mapping was done by energy dispersive X-ray spectroscopy (EDX) at 10 keV, frame dwell time 1048 s (X-Max detector, SATW window) to study the distribution of elements across the films. The phase compositions of these samples were studied using X-ray diffraction (XRD, powder diffractometer Rigaku Miniflex 600) with monochromatic Cu Kα irradiation ($\lambda = 1.5406$ Å), and the spectra were analysed using PDXL2 software. The chemical composition of synthesized material was confirmed with X-ray photoelectron spectroscopy (XPS) measurements performed using an X-ray photoelectron spectrometer ESCALAB Xi (ThermoFisher). Al Kα X-ray tube with the energy of 1486 eV was used as an excitation source, the size of the analysed sample area was 650 μm x 100 μm and the angle between the analyser and the sample surface was 90°. Sample area of interest (2x2 mm) was sputter-cleaned for 30 seconds prior to the measurements with argon ion gun (monoatomic $Ar^+$ ions with 1000 eV energy). An electron gun was used to perform charge compensation. The base pressure during spectra acquisition was better than $10^{-5}$ Pa.

## 3. RESULTS AND DISCUSSION

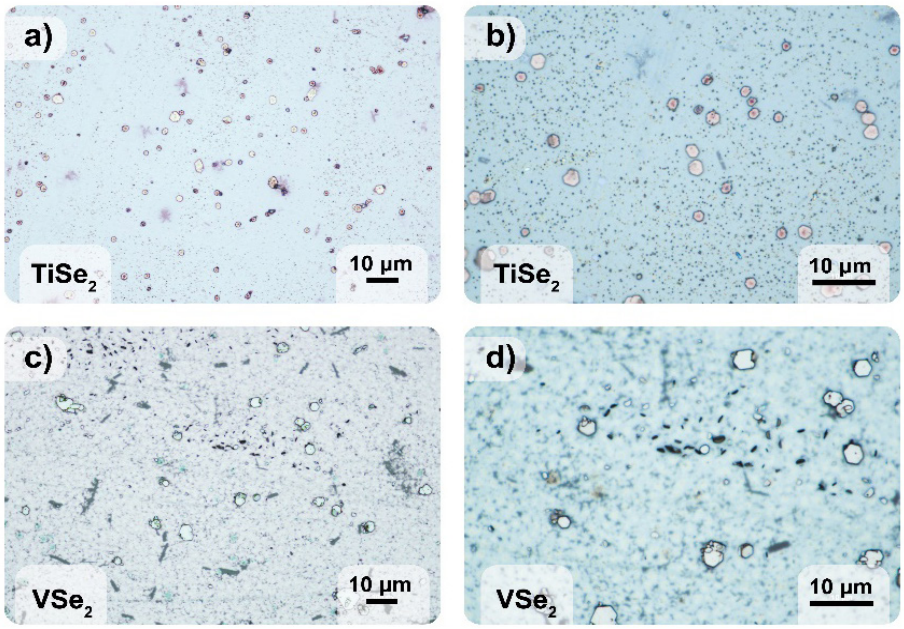


*Fig. 2.* Optical images of $TiSe_2$ (a, b) and $VSe_2$ (c, d) thin films converted at 700 °C with different magnifications, used to confirm the presence of surface crystals indicating a successful conversion of metal precursor films to their respective diselenide material.

From our experiments, 15 nm thickness of metal precursor showed continuous films of diselenide material after the selenization process, so the thickness was kept constant for all the samples involved in this study. During our experiments, initially when ampoules were made without their respective metal chips (Ti / V), some of the excess selenium vapour was noticed to have condensed near the edges of the samples where substrate touched ampoule walls, or in some cases, droplets of condensed Se were noticed on top of the synthesized material. To avoid any issues related to excess Se, extra metal chips were introduced after a few trials, which solved our issues and gave the best results. It is worth mentioning here that Ti / V film selenization attempt using elemental Se in quartz tube in gas flow at atmospheric pressure did not initiate the desired chemical reaction between Ti / V and Se in the same range of temperatures. After the process of selenization in ampoules, optical images were taken to observe the general surface area of the films (Fig. 2), which were also complimented by SEM images with a closer look at them. Figure 3 shows the SEM and XRD data obtained from TiSe2 films, and there is a visible difference in surface morphology between the samples synthesized at different temperatures. Comparing images (Fig. 3a, b, c), the sample converted at 650 °C shows coarse looking surface with quite many random comparatively big crystals of TiSe2 dispersed across the film. As we move to higher temperatures, 700 °C and 750 °C, we can see the films getting comparatively smoother. It becomes clearer when we observe images (Fig. 3d, e, f) with closer look of these films, the difference is strong in terms of average crystal sizes

and the films underneath. TiSe2 converted at 650 °C seems to have big crystals growing >2µm in size measured from edge to edge, and as we go for higher temperature of 700 °C, this size becomes <2µm and it decreases even further down to <1µm for 750 °C film. Furthermore, when we look at the overall film under these surface crystals, it seems that the film converted at 650 °C has uneven thickness of the material making islands and growing big crystals on top, but as we increase the temperature towards 750 °C, these big crystals seem to have sublimated, and the film underneath has grown to have better consistency in thickness. To assess if any of these visible differences mentioned earlier from SEM images give any variations when measured with XRD, the retrieved patterns have been also put together for comparison in Fig. 3g. The obtained data were checked with ICDD #01-083-0980 PDF card to confirm the material composition which supported our findings, and then samples prepared at different variations were compared. No drastic variations in the peak positions or width of those peaks were found. Only minor changes in peak intensity were observed, which gave weak correlation to material sublimation at higher temperature leaving thinner films producing reduced intensity of the TiSe2 peaks. Similarly, SEM and XRD data were also obtained for our synthesized films of VSe2 as shown in Fig. 4. When comparing the film morphology for VSe2 films through SEM images, films look rather similar from a larger scale (Fig. 4 a, b, c) across all temperatures, but when observed on a smaller scale (Fig. 4 d, e, f), film synthesized at 650 °C stands out with many out-of-plane crystals with protruding nanocrystals to give the film a rough profile. At 700 °C and 750 °C, the films still have ~5 µm size surface crystals but the film itself no longer has these nanocrystals, giving the film a smoother profile comparatively. To confirm the material phase, measured XRD data were compared with ICDD #04-007-5442 PDF card, which supported successful synthesis of VSe2 thin films, while showing significant difference in XRD peak intensity for VSe2 thin films synthesized at 650 °C and 700 °C, where small peak intensity was measured for 650 °C indicating smaller crystallite size (Fig. 4g). No significant difference was found between 700 °C and 750 °C.

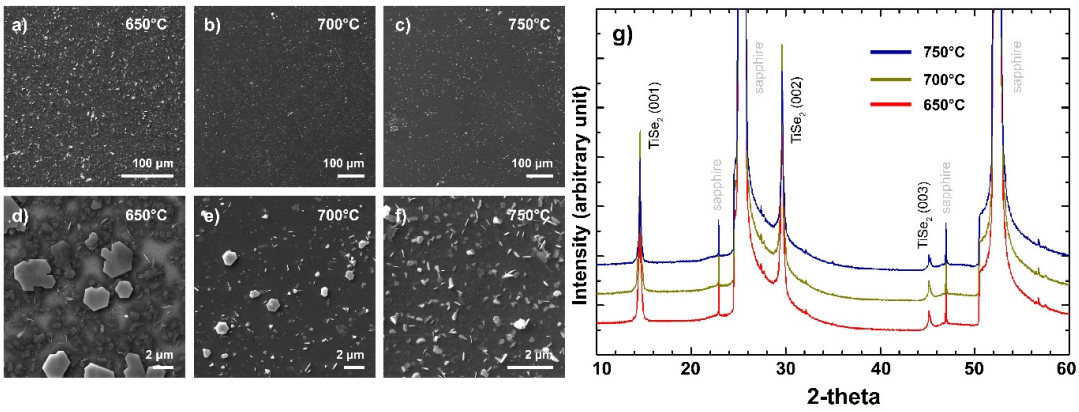


*Fig. 3.* SEM images of $TiSe_2$ thin films (a, d) converted at 650 °C (b, e), at 700 °C and (c, f) at 750 °C; (g) XRD spectra of $TiSe_2$ thin films synthesized using different temperatures.

To understand the distribution of elements across the films, EDX measurements were performed (Fig. 5) for films synthesized at 650 °C of both materials. As for $TiSe_2$ film, it seems to have higher intensity for both elements (Ti, Se) in the places of surface crystals, indicating concentrated material, which is to be expected from such top view analysis method as we observed these crystals to grow on top of the films making the material concentration higher in that place compared to rest of the film area where there were no crystals on top. Similar trend can be observed for the $VSe_2$ film as well, which has many surface crystals with comparatively smaller size. The atomic ratio of the elements was found to be roughly 1:2 for Ti / V and Se respectfully, which indicates proper stoichiometry among the crystalline planes.

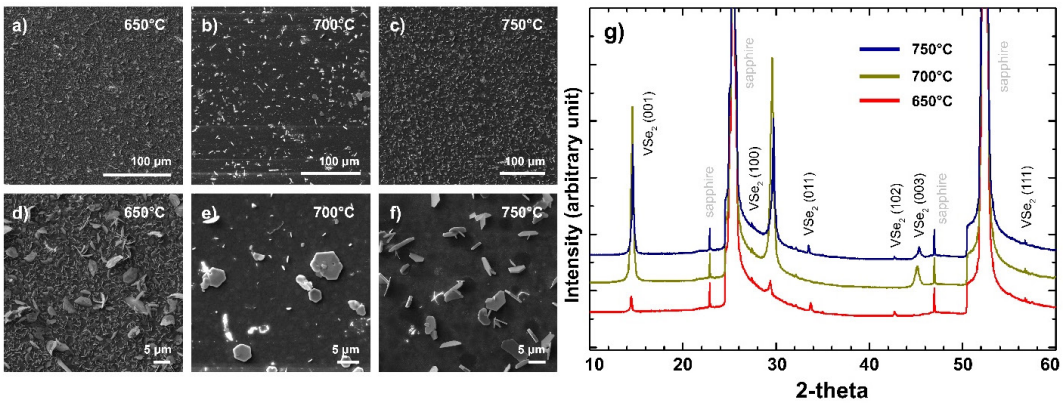


*Fig. 4.* SEM images of $VSe_2$ thin films (a, d) converted at 650 °C, (b, e), at 700 °C and (c, f) at 750 °C; (g) XRD spectra of synthesized $VSe_2$ thin films using different temperatures.

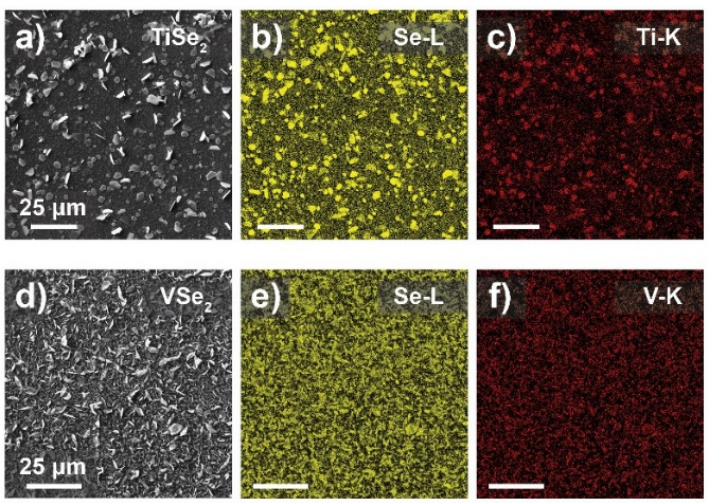


*Fig. 5.* EDX elemental mapping of (a–c) $TiSe_2$ and (d–f) $VSe_2$ films synthesized at 650 °C shows presence and distribution of their respective elements across the film.

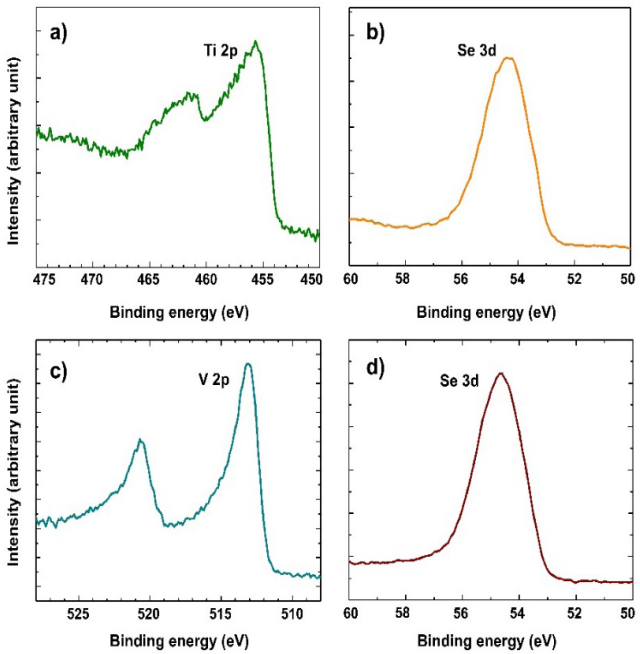


*Fig. 6.* High-resolution XPS spectra of the $TiSe_2$ synthesized at 650 °C film constituent elements for (a) Ti, and (b) Se and for $VSe_2$ film constituent elements (c) V and (d) Se.

Furthermore, XPS analysis was performed to verify the chemical states of the constituent elements in the films (Fig. 6a, b). High-resolution spectra were acquired and calibrated relative to the adventitious C 1s peak at 284.8 eV. Regarding the $TiSe_2$ films, Ti $2p_{3/2}$ peak was located at approximately 455.7 eV[34,40](spin-orbit splitting $\Delta_{3/2\ -\ 1/2}$ = 5.7 eV), matching the chemical state in $TiSe_2$ compound. Each of the spin-orbit components has an additional shoulder towards the higher binding energy, which could be attributed to a possible formation of surface oxide due to the post-synthesis exposure to air[41,42]. The Se $3d_{5/2}$ peak was located at 54.2 eV (spin-orbit splitting $\Delta_{5/2\ -\ 3/2}$ = 0.86 eV), which corresponded to the $TiSe_2$ compound [34] . Similarly, high-resolution V 2p and Se 3d peaks for $VSe_2$ were acquired (Fig. 6c, d). V $2p_{3/2}$ peak was located at 513.1 eV (spin-orbit splitting $\Delta_{3/2-1/2}$ = 7.5 eV), while the Se $3d_{5/2}$ peak was measured to be at 54.5 eV, corresponding to chemical states in $VSe_2$[43].

## 4. CONCLUSIONS

Large-area synthesis of $TiSe_2$ and $VSe_2$ using a 2-step process was investigated, and to prove the quality of synthesized materials, films were analysed using SEM, EDX, XRD and XPS techniques. Investigation of surface morphology through SEM revealed presence of hexagonal crystals on top for both materials, which varied in size and numbers depending on their synthesis temperatures, but more importantly SEM revealed that both material films remained continuous after their selenization process regardless of the temperature used. XRD patterns, also supported by XPS analysis, confirmed the composition of our synthesized materials and suggested that both the

surface crystals (visible in SEM images) and the films underneath contained our desired materials $TiSe_2$ and $VSe_2$.

According to XRD data, crystalline $TiSe_2$ can be successfully synthesized in the temperature range of 650 °C–750 °C, while $VSe_2$ – in the temperature range of 700 °C–750 °C. Using elemental mapping by EDX showed surface crystals contributing to higher material concentration in their local spots, while rest of the film area seemed to have identical levels of intensity confirming the continuity of the films further. With our demonstrated methodology, the materials can be deposited on nanostructured substrates (e.g., forest of nanowires), which would increase their surface area drastically and enhance applicability in catalytic and HER applications. This approach can be extended to synthesize other TMDs as well in large areas and create continuous films on various surfaces and even fabricate functional heterostructures.

## ACKNOWLEDGEMENTS

The research has been funded by Latvian Council of Science project (No. lzp-2020/1-0261). The Institute of Solid State Physics, University of Latvia (Latvia), as the Centre of Excellence has received funding from the European Union's Horizon 2020 Framework Programme H2020-WIDESPREAD01-2016-2017-Teaming Phase2 under grant agreement no. 739508, project CAMART2.

## REFERENCES

1. Duo, Y., Luo, G., Li, Z., Chen, Z., Li X., Jiang, Z., … & Yu, X.-F. (2021). Photothermal and Enhanced Photocatalytic Therapies Conduce to Synergistic Anticancer Phototherapy with Biodegradable Titanium Diselenide Nanosheets. *Small, 17* (40). DOI:10.1002/smll.202103239
2. Han, G. H., Duong, D. L., Keum, D. H., Yun, S. J., & Lee, Y. H. (2018). Van der Waals Metallic Transition Metal Dichalcogenides. *Chem Rev., 118* (13), 6297–6336. DOI:10.1021/acs.chemrev.7b00618
3. Goli, P., Khan, J., Wickramaratne, D., Lake, R.K., & Balandin, A.A. (2012). Charge Density Waves in Exfoliated Films of van der Waals Materials: Evolution of Raman Spectrum in TiSe2. *Nano Lett., 12* (11), 5941–5945. DOI:10.1021/nl303365x
4. Gu, Y., Katsura, Y., Yoshino, T., Takagi, H., & Taniguchi, K. (2015). Rechargeable Magnesium-Ion Battery Based on a TiSe2-Cathode with d-p Orbital Hybridized Electronic Structure. *Sci Rep., 5*. DOI:10.1038/srep12486
5. Zhang, D., Zhao, G., Li, P., Zhang, Y., Qiu, W., Shu, J. … & Sun. W. (2018). Readily Exfoliated TiSe2 Nanosheets for High-Performance Sodium Storage. *Chemistry – A European Journal, 24* (5), 1193–1197. DOI:10.1002/chem.201704661
6. Wen, L., Wu, Y., Wang, S., Shi, J., Zhang, Q., Zhao, B., … & Gao, Y. (2022). A Novel TiSe2 (De)Intercalation Type Anode for Aqueous Zinc-Based Energy Storage. *Nano Energy, 93*, 106896. DOI:10.1016/j.nanoen.2021.106896
7. Duong, D.L., Ryu, G., Hoyear, A., Lin, C., Burghard, M., & Kern, K. (2017). Raman Characterization of the Charge Density Wave Phase of 1T-TiSe2: From Bulk to Atomically Thin Layers. *ACS Nano,11* (1), 1034–1040. DOI:10.1021/acsnano.6b07737
8. Lian, C., Zhang, S.J., Hu, S.Q., Guan, M.X., & Meng, S. (2020). Ultrafast Charge

Ordering by Self-Amplified Exciton–Phonon Dynamics in TiSe2. *Nat Commun., 11* (1). DOI:10.1038/s41467-019-13672-7

9. Yu, W., Li, J., Herng, T.S., Wang, Z., Zhao, X., Chi, X., … & Loh, K. P. (2019). Chemically Exfoliated VSe2 Monolayers with Room-Temperature Ferromagnetism. *Advanced Materials, 31* (40). DOI:10.1002/adma.201903779
10. Li, F., Tu, K., & Chen, Z. (2014). Versatile Electronic Properties of VSe2 Bulk, Few-Layers, Monolayer, Nanoribbons, and Nanotubes: A Computational Exploration. *Journal of Physical Chemistry C, 118* (36), 21264–21274. doi:10.1021/jp507093t
11. Snow, C. S., Karpus, J. F., Cooper, S. L., Kidd, T. E., & Chiang, T. C. (2003). Quantum Melting of the Charge-Density-Wave State in 1T-TiSe2. *Phys Rev Lett., 91* (13), 1364021–1364024. DOI:10.1103/physrevlett.91.136402
12. Kolekar, S., Bonilla, M., Ma, Y., Diaz, H. C., & Batzill, M. (2018). Layer- and Substrate-Dependent Charge Density Wave Criticality in 1T-TiSe2. *2d Mater., 5* (1). DOI:10.1088/2053-1583/aa8e6f
13. Zhu, X., Cao, Y., Zhang, J., Plummer, E. W., & Guo, J. (2015). Classification of Charge Density Waves Based on their Nature. *Proc Natl Acad Sci U S A, 112* (8), 2367–2371. DOI:10.1073/pnas.1424791112
14. Rossnagel, K. (2011). On the Origin of Charge-Density Waves in Select Layered Transition-Metal Dichalcogenides. *Journal of Physics Condensed Matter, 23* (21). DOI:10.1088/0953-8984/23/21/213001
15. Feng, J., Biswas, D., Rajan, A., Watson, M. D., Mazzola, F., Clark, O. J., … & King, P. D. C. (2018). Electronic Structure and Enhanced Charge-Density Wave Order of Monolayer VSe2. *Nano Lett., 18* (7), 4493–4499. DOI:10.1021/acs.nanolett.8b01649
16. Sugawara, K., Nakata, Y., Shimizu, R., Han, P., Hitosugi, T., Sato, T., & Takahashi, T. (2016). Unconventional Charge-Density-Wave Transition in Monolayer 1T-TiSe2. *ACS Nano, 10* (1), 1341–1345. DOI:10.1021/acsnano.5b06727
17. Wang, H., Chen, Y., Duchamp, M., Zeng, Q., Wang, X., Tsang, S. H., … & Liu, Z. (2018). Large-Area Atomic Layers of the Charge-Density-Wave Conductor TiSe2. *Advanced Materials, 30* (8). DOI:10.1002/adma.201704382
18. Chen, P., Chan, Y.-H., Fang, X.-Y., Chou, M. Y., Mo, S.-K., Hussain, Z., … & Chiang, T.-C. (2015). Charge Density Wave Transition in Single-Layer Titanium Diselenide. *Nat Commun., 6*, 8943. DOI:10.1038/ncomms9943
19. Chen, P., Chan, Y.-H., Wong, M.-H., Fang, X.-Y., Chou, M. Y., Mo., S.-K., … & Chiang, T.-C. (2016). Dimensional Effects on the Charge Density Waves in Ultrathin Films of TiSe2. *Nano Lett., 16* (10), 6331–6336. DOI:10.1021/acs.nanolett.6b02710
20. Otto, M. R., Pöhls, J. H., René de Cotret L. P., Stern, M. J., Sutton, M., & Siwick, B. J. (2021). Mechanisms of Electron-Phonon Coupling Unraveled in Momentum and Time: The Case of Soft Phonons in TiSe 2. *Science Advances, 7* (20). http://advances.sciencemag.org/
21. Kumar, A., Sharma, R., Yadav, S., Swami, S. K., Kumari, R., Singh, V. N., … & Sinha, O. P. (2021). A Study on Chemical Exfoliation and Structural and Optical Properties of Two-Dimensional Layered Titanium Diselenide. *Dalton Transactions, 50* (11), 3894–3903. DOI:10.1039/d0dt03689g
22. Luo, H., Krizan, J. W., Seibel, E. M., Xie, W., Sahasrabudhe, G. S., Bergman, S. L., … & Cava, R. J. (2015). Cr-Doped TiSe2 – A Layered Dichalcogenide Spin Glass. *Chemistry of Materials, 27* (19), 6810–6817. DOI:10.1021/acs.chemmater.5b03091
23. Peng, J. P., Guan, J.-Q., Zhang, H.-M., Song, C.-L., Wang, L., He, K., … & Ma, Z.-C.. (2015). Molecular Beam Epitaxy Growth and Scanning Tunneling Microscopy Study of TiSe2 Ultrathin Films. *Phys Rev B Condens Matter Mater Phys., 91* (12). DOI:10.1103/PhysRevB.91.121113
24. Liao, M., Wang, H., Zhu, Y., Shang, R., Rafique, M., Yang, L., … & Xue, Q.-K. (2021). Coexistence of Resistance Oscillations and the Anomalous Metal Phase in a Lithium Intercalated TiSe2 Superconductor. *Nat Commun., 12* (1). DOI:10.1038/s41467-021-25671-8

25. Sree Raj, K. A., Shajahan, A. S., Chakraborty, B., & Rout, C. S. (2020). Two-Dimensional Layered Metallic VSe2/SWCNTs/rGO Based Ternary Hybrid Materials for High Performance Energy Storage Applications. *Chemistry - A European Journal*, *26* (29), 6662–6669. DOI:10.1002/chem.202000243
26. Ming, F., Liang, H., Lei, Y., Zhang, W., & Alshareef, H. N. (2018). Solution Synthesis of VSe2 Nanosheets and their Alkali Metal Ion Storage Performance. *Nano Energy, 53*, 11–16. DOI:10.1016/j.nanoen.2018.08.035
27. Oliveira, C. C., & Autreto P. A. (2023). Optimized 2D Nanostructures for Catalysis of Hydrogen Evolution Reactions. *MRS Advances, 8* (6), 307–310. DOI:10.1557/s43580-023-00549-7
28. Yan M., Pan, X., Wang, P., Chen, F., He, L., Jiang, G., … & Mai, L. (2017). Field-Effect Tuned Adsorption Dynamics of $VSe_2$ Nanosheets for Enhanced Hydrogen Evolution Reaction. *Nano Lett., 17* (7), 4109-4115. DOI:10.1021/acs.nanolett.7b00855
29. Yan, M., Pan, X., Wang, P., Chen, F., He, L., Jiang, G., ... & Mai, L. (2017). Field-Effect Tuned Adsorption Dynamics of VSe2 Nanosheets for Enhanced Hydrogen Evolution Reaction. *Nano Letters, 17* (7), 4109-4115. DOI: 10.1021/acs.nanolett.7b00855
30. Fu, J., Ali, R., Mu, C., Liu, Y., Mahmood, N., Lau, W.-M., & Jian, X. (2021). Large-Scale Preparation of 2D VSe2 through a Defect-Engineering Approach for Efficient Hydrogen Evolution Reaction. *Chemical Engineering Journal, 411*, 128494. DOI:10.1016/j.cej.2021.128494
31. Song, Z., Yi, J., Qi, J., Zheng, Q., Zhu, Z., Tao, L. …, & Gao, H.-J. (2022). Line Defects in Monolayer $TiSe_2$ with Adsorption of Pt Atoms Potentially Enable Excellent Catalytic Activity. *Nano Res., 15* (5), 4687–4692. DOI:10.1007/s12274-021-4002-y
32. Toh, R. J., Sofer, Z., & Pumera, M. (2016). Catalytic Properties of Group 4 Transition Metal Dichalcogenides (MX2; M = Ti, Zr, Hf; X = S, Se, Te). *J Mater Chem A Mater.*, *4* (47), 18322–18334. DOI:10.1039/c6ta08089h
33. Huang, H. H., Fan, X., Singh, D. J., & Zheng, W. T. (2020). Recent Progress of TMD Nanomaterials: Phase Transitions and Applications. *Nanoscale, 12* (3), 1247–1268. DOI:10.1039/c9nr08313h
34. Chowdhury, T., Sadler, E. C., & Kempa, T. J. Progress and Prospects in Transition-Metal Dichalcogenide Research beyond 2D. *Chem Rev.*, *120* (22), 12563–12591. DOI:10.1021/acs.chemrev.0c00505
35. Chhowalla, M., Liu, Z., & Zhang, H. (2015). Two-dimensional Transition Metal Dichalcogenide (TMD) Nanosheets. *Chem Soc Rev., 44* (9), 2584–2586. DOI:10.1039/c5cs90037a
36. Pasquier, D., & Yazyev, O. V. (2018). Excitonic Effects in Two-dimensional $TiSe_2$ from Hybrid Density Functional Theory. *Phys Rev B., 98* (23). DOI:10.1103/PhysRevB.98.235106
37. Kadiwala, K., Butanovs, E., Ogurcovs, A., Zubkins, M., & Polyakov, B. (2022). Comparative Study of $WSe_2$ Thin Films Synthesized via Pre-deposited WO3 and W Precursor Material Selenization. *J Cryst Growth., 593*. DOI:10.1016/j.jcrysgro.2022.126764
38. Kwak, T., Lee, J., So, B., Choi, U., & Nam, O. (2019). Growth Behavior of Wafer-Scale Two-dimensional MoS 2 Layer Growth Using Metal-Organic Chemical Vapor Deposition. *J Cryst Growth, 510,* 50–55. DOI:10.1016/j.jcrysgro.2019.01.020
39. Xue, Y., Zhang, Y., Wang, H., Lin, S., Li, Y., Dai, J.-Y., & Lau, S. P. (2020). Thickness-Dependent Magnetotransport Properties in 1T $VSe_2$ Single Crystals Prepared by Chemical Vapor Deposition. *Nanotechnology, 31* (14), 145712. DOI:10.1088/1361-6528/ab6478